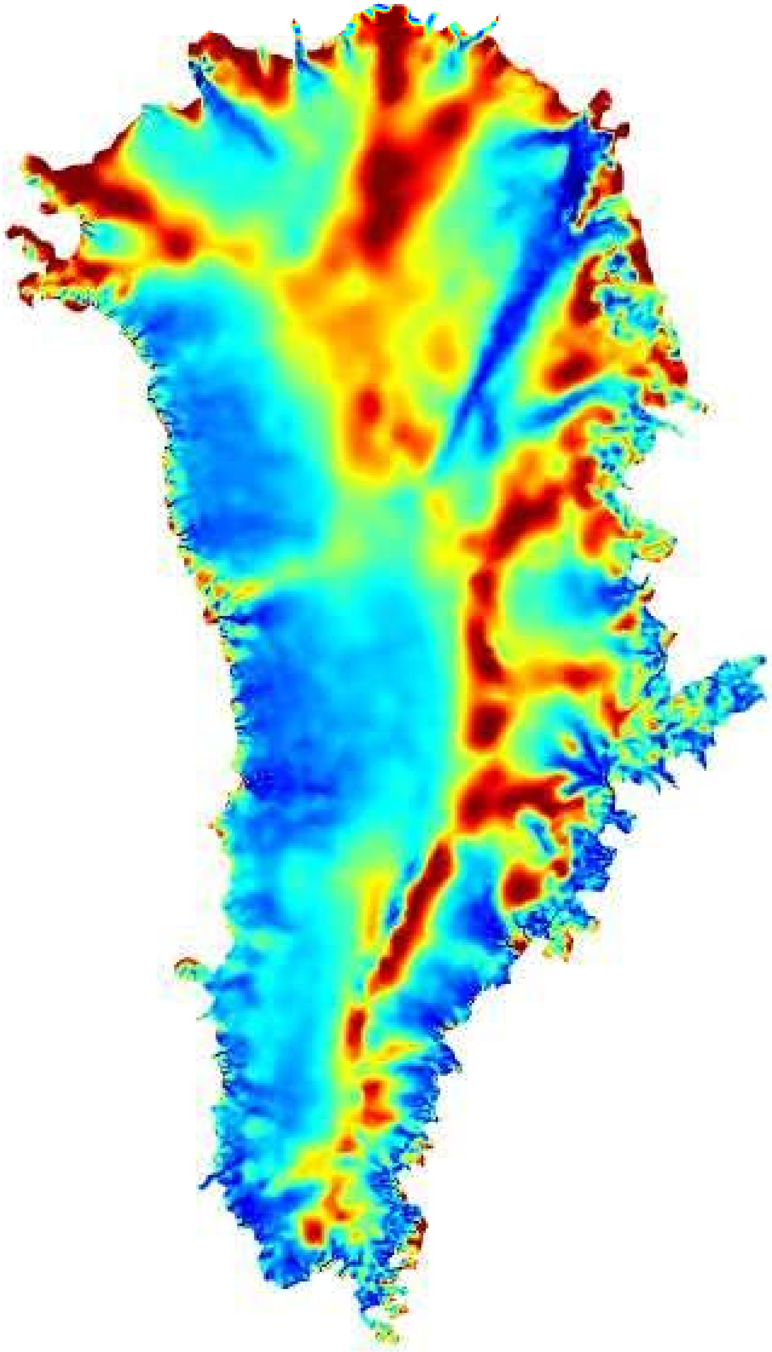

Multifidelity Proper Orthogonal Decomposition

Conference on Mathematical and Applied Aspects of Complexity Reduction Methods

In honor of the Chair of Yvon Maday
Collège de France, Paris
June 24, 2026

Professor Karen E. Willcox
Director, Oden Institute for Computational Engineering & Sciences
Professor of Aerospace Engineering & Engineering Mechanics
University of Texas at Austin

Motivation

Proper orthogonal decomposition (POD) is a workhorse of dimension reduction and reduced-order modeling.

But the computational cost of generating training snapshots is often prohibitive.

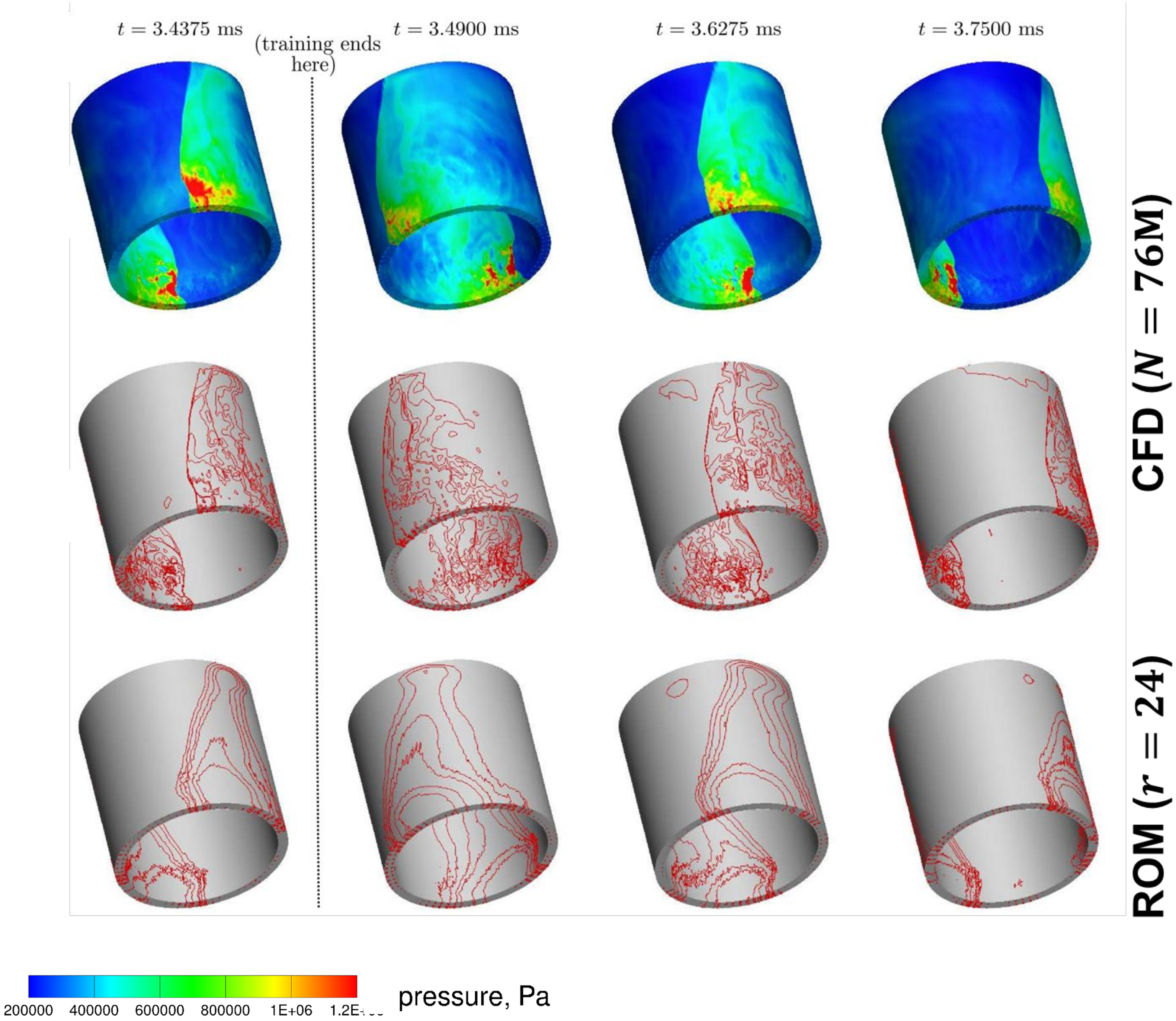

Motivation

We draw inspiration from multifidelity UQ methods, which leverage approximate models to reduce the cost of sampling.

Aretz, Gunzburger, Morlighem & W. Multifidelity UQ for ice sheet simulations. *Computational Geosciences*, 2025.

Uncertainty in basal friction field

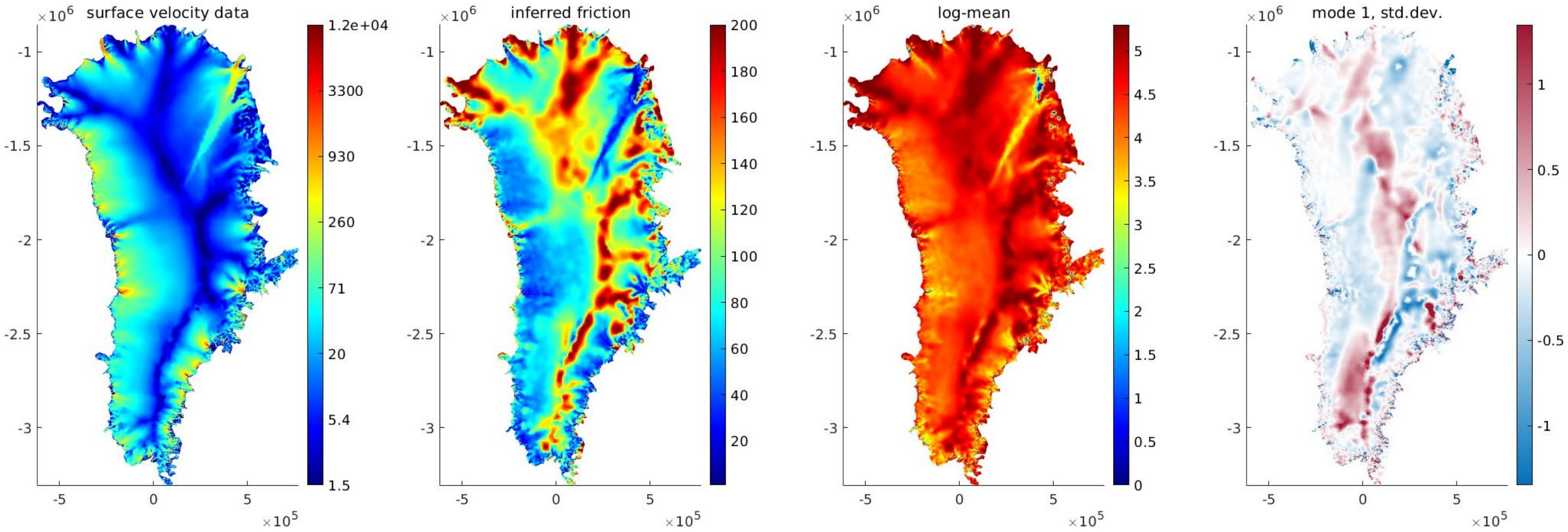

Uncertainty in geothermal heat flux

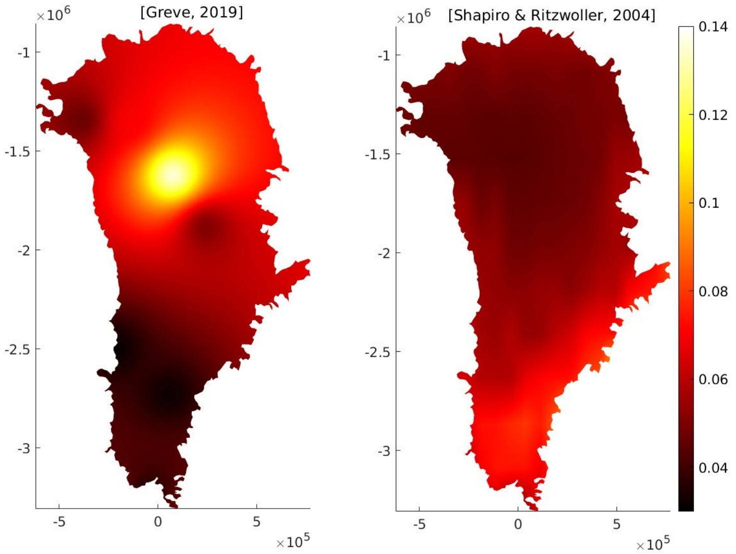

Uncertainty in estimated ice thickness

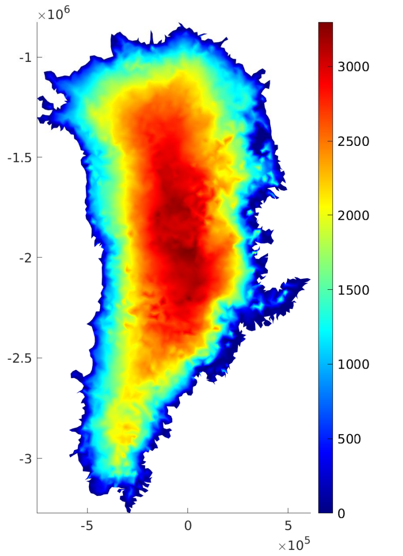

Proper Orthogonal Decomposition

- Consider m **snapshots** $\boldsymbol{u}_1, \boldsymbol{u}_2, \ldots, \boldsymbol{u}_m \in \mathbb{R}^n$ (solutions at selected times or parameter values)

- Form the snapshot matrix $\mathbf{U} = [\boldsymbol{u}_1 \;\; \boldsymbol{u}_2 \;\; \ldots \;\; \boldsymbol{u}_m] \in \mathbb{R}^{n \times m}$

- Choose the r basis vectors $\mathbf{V} = [\boldsymbol{v}_1 \; \boldsymbol{v}_2 \;\; \ldots \boldsymbol{v}_r]$ to be left **singular vectors** of the snapshot matrix, with singular values

$$\sigma_1 \geq \sigma_2 \geq \cdots \geq \sigma_r \geq \sigma_{r+1} \geq \cdots \geq \sigma_m \geq 0$$

- This is the optimal projection in a least squares sense:

$$\boxed{\min_{\mathbf{V}^\top \mathbf{V} = \mathbf{I}} \sum_{i=1}^{m} \|\boldsymbol{u}_i - \mathbf{V}\mathbf{V}^\top \boldsymbol{u}_i\|_2^2 = \sum_{i=r+1}^{m} \sigma_i^2}$$

Proper Orthogonal Decomposition

POD basis vectors are:

- the left singular vectors of the snapshot matrix
  $\mathbf{U} = [\boldsymbol{u}_1 \;\; \boldsymbol{u}_2 \; \ldots \; \boldsymbol{u}_m]$

- the eigenvectors of $\mathbf{U}\mathbf{U}^\top$

$$\mathbf{U}\mathbf{U}^\top = \sum_{i=1}^{m} \boldsymbol{u}_i \boldsymbol{u}_i^\top \qquad (n \times n)$$

- linear combinations of the snapshots:
  $\mathbf{W}\mathbf{U}$, where $\mathbf{W}$ are the eigenvectors of $\mathbf{U}^\top\mathbf{U}$

$$\mathbf{U}^\top\mathbf{U} = \sum_{i=1}^{m} \boldsymbol{u}_i^\top \boldsymbol{u}_i \qquad (m \times m)$$

Proper Orthogonal Decomposition

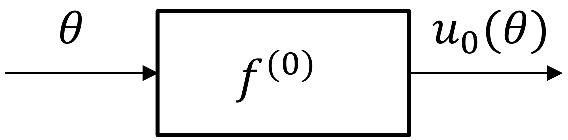

high-fidelity model $f^{(0)}$ maps parameter θ to state $u_0(\theta)$ with computational cost c_0

$$V = \underset{V \subset H, \dim V = r}{\arg\min} \frac{1}{m} \sum_{i=1}^{m} \|u_0(\theta_i) - \Pi_V u_0(\theta_i)\|_H^2$$

Consider input parameters $\theta \sim \mu$; draw m i.i.d. samples $\theta_1, \theta_2, \dots, \theta_m$

Generate m snapshots $u_0(\theta_1), u_0(\theta_2), \dots, u_0(\theta_m)$; computational cost $c_{\text{tot}} = mc_o$

POD cost function $$\mathcal{J}_{\text{mc}}(V) := \frac{1}{m} \sum_{i=1}^{m} \|u_0(\theta_i) - \Pi_V u_0(\theta_i)\|_H^2$$

is Monte Carlo approximation of $$\mathcal{J}(V) := \mathbb{E}_{\theta \sim \mu}\left[\|u_0(\theta) - \Pi_V u_0(\theta)\|_H^2\right]$$

Proper Orthogonal Decomposition

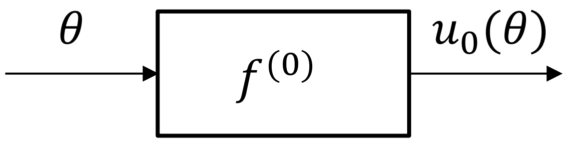

high-fidelity model maps parameter θ to state $u_0(\theta)$ with computational cost c_0

$$V = \underset{V \subset H, \dim V = r}{\arg\min} \frac{1}{m} \sum_{i=1}^{m} \|u_0(\theta_i) - \Pi_V u_0(\theta_i)\|_H^2$$

Monte Carlo approximation of $\mathcal{J}(V) := \mathbb{E}_{\theta \sim \mu}\left[\|u_0(\theta) - \Pi_V u_0(\theta)\|_H^2\right]$

has mean squared error

$$\mathrm{MSE}[\mathcal{J}_{\mathrm{mc}}(V)] := \mathbb{E}_{\theta_1, \ldots, \theta_m \sim \mu}\left[(\mathcal{J}_{\mathrm{mc}}(V) - \mathcal{J}(V))^2\right] = \frac{1}{m} \mathbb{V}_{\theta \sim \mu}(\|u_0(\theta) - \Pi_V u_0(\theta)\|_H^2)$$

Multifidelity Monte Carlo
Variance reduction via control variates

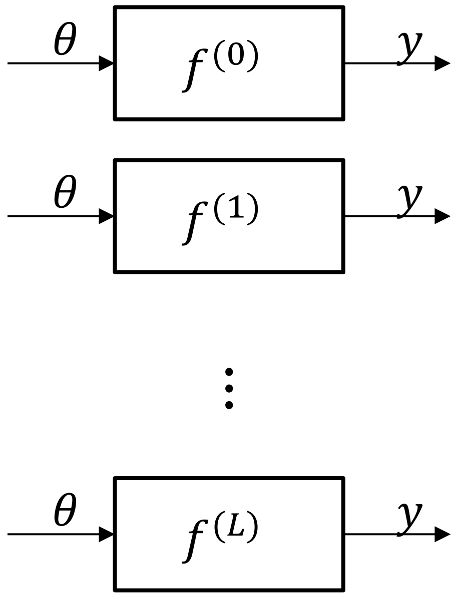

- model $f^{(\ell)}$ has cost c_ℓ
- m_ℓ evaluations for model ℓ, with

$$m_0 \leq m_1 \leq \ldots \leq m_L$$

- MFMC estimator of $\mathbb{E}[y]$:

$$\hat{s} = \bar{y}^{(0)}_{m_0} + \sum_{\ell=1}^{L} \alpha_\ell \left(\bar{y}^{(\ell)}_{m_\ell} - \bar{y}^{(\ell)}_{m_{\ell-1}} \right)$$

MFMC estimate for the mean

mean estimate using m_0 evaluations of truth model

mean estimate using m_ℓ evaluations of modelℓ

mean estimate using $m_{\ell-1}$ evaluations of modelℓ

Ng & W. AIAA 2012, IJNME 2014
Peherstorfer, W, Gunzburger, SISC 2016

Multifidelity Monte Carlo
Variance reduction via control variates

MFMC estimator

$$\hat{s} = \bar{y}^{(0)}_{m_0} + \sum_{\ell=1}^{L} \alpha_\ell \left(\bar{y}^{(\ell)}_{m_\ell} - \bar{y}^{(\ell)}_{m_{\ell-1}} \right)$$

MFMC estimate for the mean

mean estimate using m_0 evaluations of truth model

mean estimate using m_i evaluations of model i

mean estimate using m_{i-1} evaluations of model i

MFMC estimator is **unbiased**, even with no error bounds for surrogates: $E[\hat{s}] = s$

MSE is: $$\mathrm{Var}[\hat{s}] = \frac{\sigma_0^2}{m_0} + \sum_{\ell=1}^{L} \left(\frac{1}{m_{\ell-1}} - \frac{1}{m_\ell} \right) \left(\alpha_\ell^2 \sigma_\ell^2 - 2\alpha_\ell \rho_\ell \sigma_\ell \sigma_0 \right)$$

- σ_ℓ^2 is variance of $f^{(\ell)}(\theta)$
- ρ_ℓ is correlation coefficient between $f^{(0)}(\theta)$ and $f^{(\ell)}(\theta)$

Ng & W. AIAA 2012, IJNME 2014
Peherstorfer, W, Gunzburger, SISC 2016

Multifidelity Monte Carlo
Variance reduction via control variates

The costs of the MFMC estimator are: $c_{\text{tot}}(\hat{s}) = \sum_{\ell=0}^{L} c_\ell m_\ell$

Minimize the MSE of the MFMC estimator for a given computational budget p:

$$\begin{aligned} \min_{m \in \mathbb{R}^{L+1}, \alpha_1, \dots, \alpha_L \in \mathbb{R}} \quad & \mathrm{Var}[\hat{s}] \\ \text{s.t.} \quad & m_{\ell-1} \leq m_\ell, \ell = 1, \dots, L \\ & 0 \leq m_0 \\ & c_{\text{tot}}(\hat{s}) = c^T m = p \end{aligned}$$

Optimal control variate coefficients: $\alpha_\ell^* = \rho_\ell \frac{\sigma_0}{\sigma_\ell}, \; \ell = 1, \dots, L$

Optimal sample sizes: $m_0^* = \frac{\gamma}{c_{\text{tot}}^{\mathrm{T}} \eta}, \; m_\ell^* = \eta_\ell m_0, \; \ell = 1, \dots, L$

$$\eta_\ell = \sqrt{\frac{c_0(\rho_\ell^2 - \rho_{\ell+1}^2)}{c_\ell(1-\rho_1^2)}} \qquad \ell = 1, \dots, L$$

Peherstorfer, W, Gunzburger, SISC 2016

Let’s come back to POD

Multifidelity POD

Variance reduction via control variates → lower snapshot cost

Define a statistically unbiased multifidelity cost function

$$\mathbb{E}[\mathcal{J}_{\mathrm{mf}}(V)] = \mathbb{E}[\mathcal{J}(V)] = \mathbb{E}_{\theta\sim\mu}[\|u_0(\theta) - \Pi_V u_0(\theta)\|_H^2]$$

with

$$\mathrm{MSE}[\mathcal{J}_{\mathrm{mf}}(V)] = \mathbb{E}[(\mathcal{J}_{\mathrm{mf}}(V) - \mathcal{J}(V))^2] \leq \mathrm{MSE}[\mathcal{J}_{\mathrm{mc}}(V)]$$

Then the mfPOD basis is given by

$$V = \operatorname*{arg\,min}_{V\subset H,\, \dim V = r} \mathcal{J}_{\mathrm{mf}}(V)$$

Multifidelity POD

Variance reduction via control variates → lower snapshot cost

$$\mathcal{J}_{mf}(V,\alpha)$$
$$= \frac{1}{m_0}\sum_{i=1}^{m_0} \|u_0(\theta_{\boldsymbol{i}}) - \Pi_V u_0(\theta_{\boldsymbol{i}})\|_{\mathrm{H}}^2$$
$$+ \sum_{\ell=1}^{L}\left(\frac{\alpha_\ell}{m_\ell}\sum_{i=1}^{m_\ell} \|u_\ell(\theta_{\boldsymbol{i}}) - \Pi_V u_\ell(\theta_{\boldsymbol{i}})\|_{\mathrm{H}}^2 - \frac{\alpha_\ell}{m_{\ell-1}}\sum_{i=1}^{m_{\ell-1}} \|u_\ell(\theta_{\boldsymbol{i}}) - \Pi_V u_\ell(\theta_{\boldsymbol{i}})\|_{\mathrm{H}}^2\right)$$

Total sampling cost for $\mathcal{J}_{mf}$ is $\sum_{\ell=0}^{L} m_\ell c_\ell$

Multifidelity POD

Variance reduction via control variates → lower snapshot cost

$$\mathrm{MSE}(\mathcal{J}_{\mathrm{mf}}(V)) = \frac{\sigma_0^2(V)}{m_0} + \sum_{\ell=1}^{L}\left(\frac{1}{m_{\ell-1}} - \frac{1}{m_\ell}\right)\left(\alpha_\ell^2\sigma_\ell^2(V) - 2\alpha_\ell\sigma_{0,\ell}(V)\right)$$

with

$$\sigma_\ell^2(V) := \mathbb{V}_{\theta\sim\mu}\left(\|u_\ell(\theta) - \Pi_V u_\ell(\theta)\|_H^2\right),$$

$$\sigma_{0,\ell}(V) := \mathrm{Cov}_{\theta\sim\mu}\left(\|u_0(\theta) - \Pi_V u_0(\theta)\|_H^2, \|u_\ell(\theta) - \Pi_V u_\ell(\theta)\|_H^2\right)$$

choosing

$$\alpha_\ell^*(V) := \begin{cases} \sigma_{0,\ell}(V)/\sigma_\ell^2(V) & \text{if } \sigma_\ell^2(V) > 0 \\ 0 & \text{if } \sigma_\ell^2(V) = 0 \end{cases}$$

yields

$$\mathrm{MSE}(\mathcal{J}_{\mathrm{mf}}(V)) = \frac{\sigma_0^2(V)}{m_0} - \sum_{\substack{\ell=1 \\ \sigma_\ell^2(V)\neq 0}}^{L}\left(\frac{1}{m_{\ell-1}} - \frac{1}{m_\ell}\right)\frac{\sigma_{0,\ell}^2(V)}{\sigma_\ell^2(V)} \leq \frac{\sigma_0^2(V)}{m_0}$$

Multifidelity POD
Theoretical results

- mfPOD correlation operator converges in probability to the POD second moment operator in the Hilbert-Schmidt norm. The rate of convergence is inversely proportional to the total snapshot sampling cost c_{tot}.
- An upper bound for the MSE of the summed mfPOD eigenvalues $\sum_{j=1}^{r} \lambda_j$ approximating $\sum_{j=1}^{r} \lambda_j^*$.
- Under the condition that $\lambda_r^* > \lambda_{r+1}^*$, an upper bound for the MSE of the summed projection error $\sum_{j=1}^{r} \left\| v_j - \Pi_{V_r^*} v_j \right\|_H^2$ of the mfPOD eigenfunctions $v_1, \dots, v_r$ onto $\mathrm{V}^* = \mathrm{span}(v_1^*, \dots, v_r^*)$.
- Both MSE upper bounds are of order $\mathcal{O}(r/c_{\mathrm{tot}})$, showing that, in the limit of arbitrarily large budget, in probability the mfPOD method recovers both the truth POD subspace V^* and its captured energy.

Algorithm 1 Discrete MFPOD

Dependencies: sampling function for probability distribution μ, snapshot evaluation functions $\theta \mapsto \mathbf{u}_0(\theta)$ and $\theta \mapsto \mathbf{u}_1(\theta)$ of the high- and low-fidelity models

Input: sample sizes $1 \leq m_0 < m_1$, weight $\alpha_1 \in \mathbb{R}$, cumulative energy threshold $0 < \kappa < 1$

`\\ step 1: snapshots`

Draw m_1 i.i.d. samples $\theta_1, \dots, \theta_{m_1} \sim \mu$

Compute high-fidelity snapshot matrix $\mathbf{S}_0 \leftarrow [\mathbf{u}_0(\theta_1), \dots, \mathbf{u}_0(\theta_{m_0})] \in \mathbb{R}^{n \times m_0}$

Compute low-fidelity snapshot matrices $\mathbf{S}_1 \leftarrow [\mathbf{u}_1(\theta_1), \dots, \mathbf{u}_1(\theta_{m_0})] \in \mathbb{R}^{n \times m_0}$ and $\mathbf{S}_+ \leftarrow [\mathbf{u}_1(\theta_{m_0+1}), \dots, \mathbf{u}_1(\theta_{m_1})] \in \mathbb{R}^{n \times (m_1 - m_0)}$

`\\ step 2: eigenvalues`

Set up matrix action $\mathbf{v} \mapsto \mathbf{C}_{\mathrm{mf}}\mathbf{v} := \frac{1}{m_0}\mathbf{S}_0(\mathbf{S}_0^\top \mathbf{v}) + (\frac{\alpha_1}{m_1} - \frac{\alpha_1}{m_0})\mathbf{S}_1(\mathbf{S}_1^\top \mathbf{v}) + \frac{\alpha_1}{m_1}\mathbf{S}_+(\mathbf{S}_+^\top \mathbf{v})$

Identify the $r_{\max} \leq m_0 + m_1$ eigenvalue-eigenvector pairs $(\lambda_j, \mathbf{v}_j) \in \mathbb{R} \times \mathbb{R}^n$, $\mathbf{C}_{\mathrm{mf}}\mathbf{v}_j = \lambda_j \mathbf{v}_j$ for which $\lambda_j \neq 0$

for $j = 1, \dots, r_{\max}$: **if** $\lambda_j > 0$ **then** $\lambda_j^+ \leftarrow \lambda_j$ **else** $\lambda_j^+ \leftarrow \frac{1}{m_0}(\mathbf{S}_0^\top \mathbf{v}_j)^\top (\mathbf{S}_0^\top \mathbf{v}_j)$

`\\ step 3: Reduced space`

Re-order $\{(\lambda_j^+, \mathbf{v}_j)\}_{j=1}^{r_{\max}}$ such that $\lambda_1^+ \geq \lambda_2^+ \geq \cdots \geq \lambda_{r_{\max}}^+ \geq 0$

Choose $r \leq r_{\max}$ minimal with $\sum_{j=1}^{r} \lambda_j^+ \geq \kappa \sum_{j=1}^{r_{\max}} \lambda_j^+$

Set $\mathbf{V} \leftarrow [\mathbf{v}_1, \dots, \mathbf{v}_r]$

return $\mathbf{V}$

Illustrative Example: 1D advection diffusion

$$-\frac{1}{\theta}\Delta u - u_x = 0 \quad \text{on } \Omega \coloneqq (0,1)$$

$$u(0) = 1, u(1) = 0$$

High fidelity FEM: 4097 dof

Low fidelity FEM: 33 dof

$\theta \sim \mathcal{U}(1,100)$

Reference: 100,000 snapshots

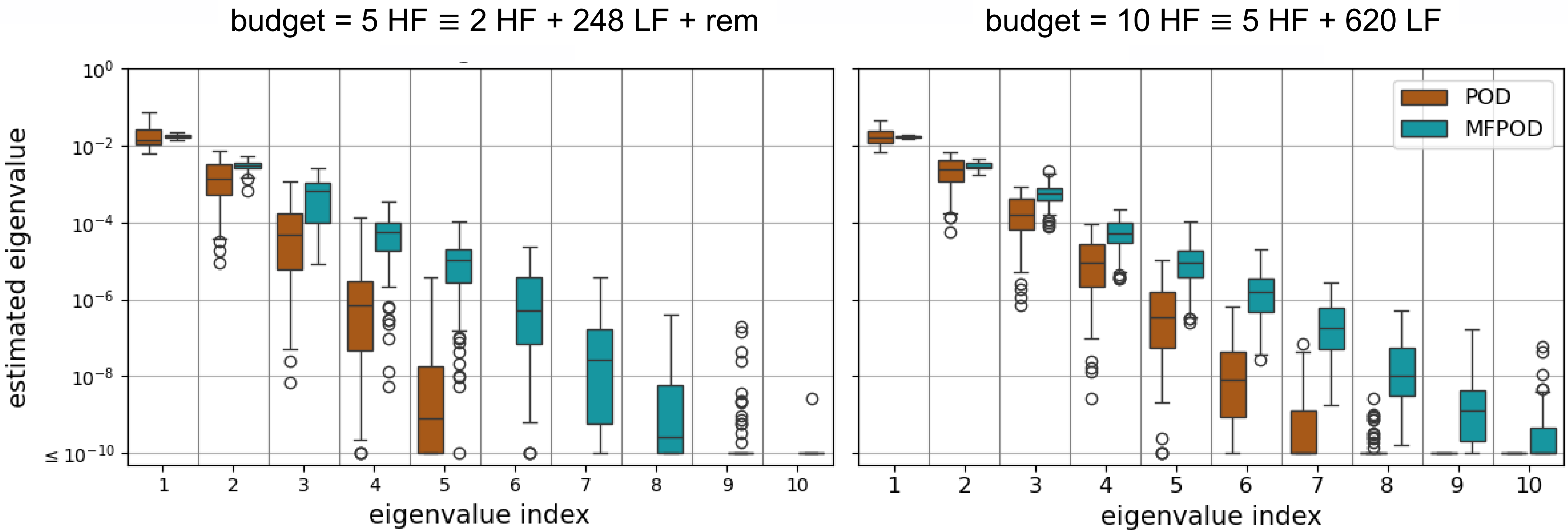

Illustrative Example: 1D advection diffusion

$$-\frac{1}{\theta}\Delta u - u_x = 0 \quad \text{on } \Omega \coloneqq (0,1)$$

$$u(0) = 1, u(1) = 0$$

High fidelity FEM: 4097 dof

Low fidelity FEM: 33 dof

$\theta \sim \mathcal{U}(1,100)$

Reference: 100,000 snapshots

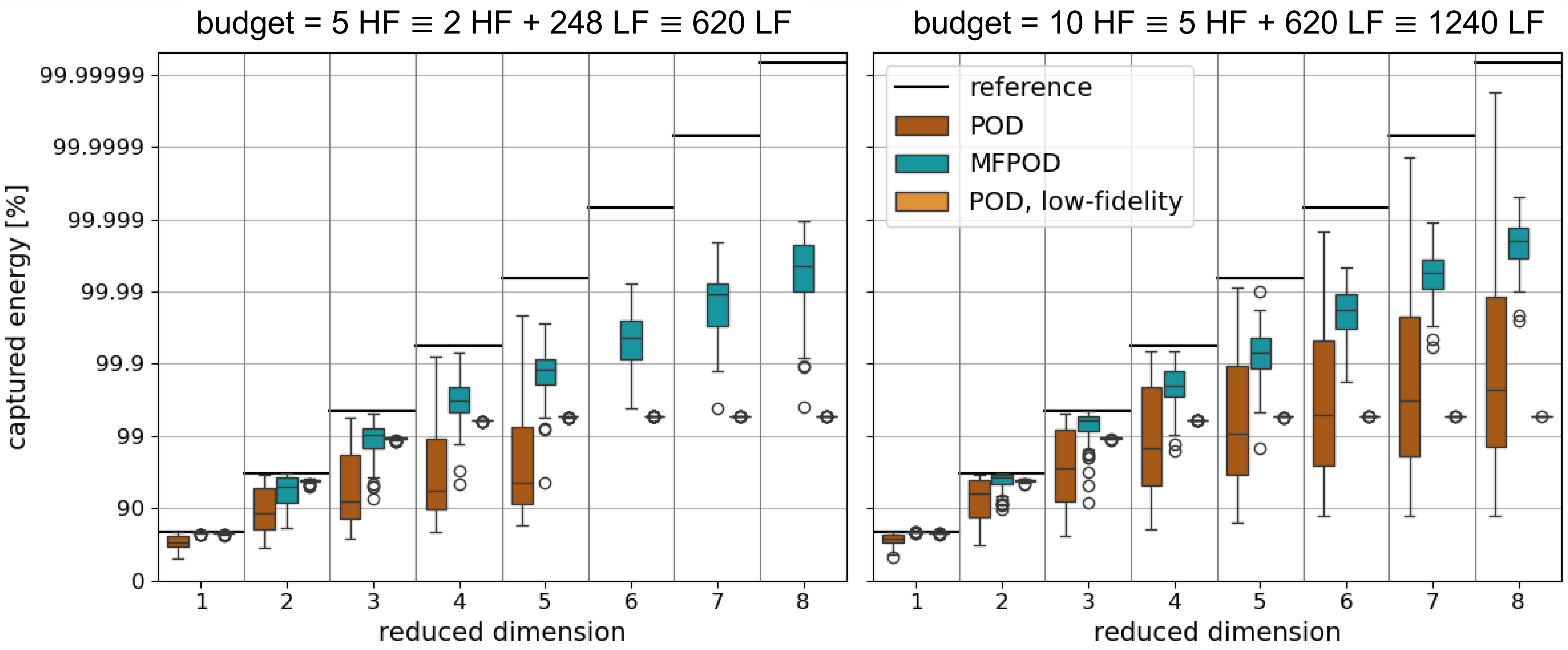

Illustrative Example: 1D advection diffusion

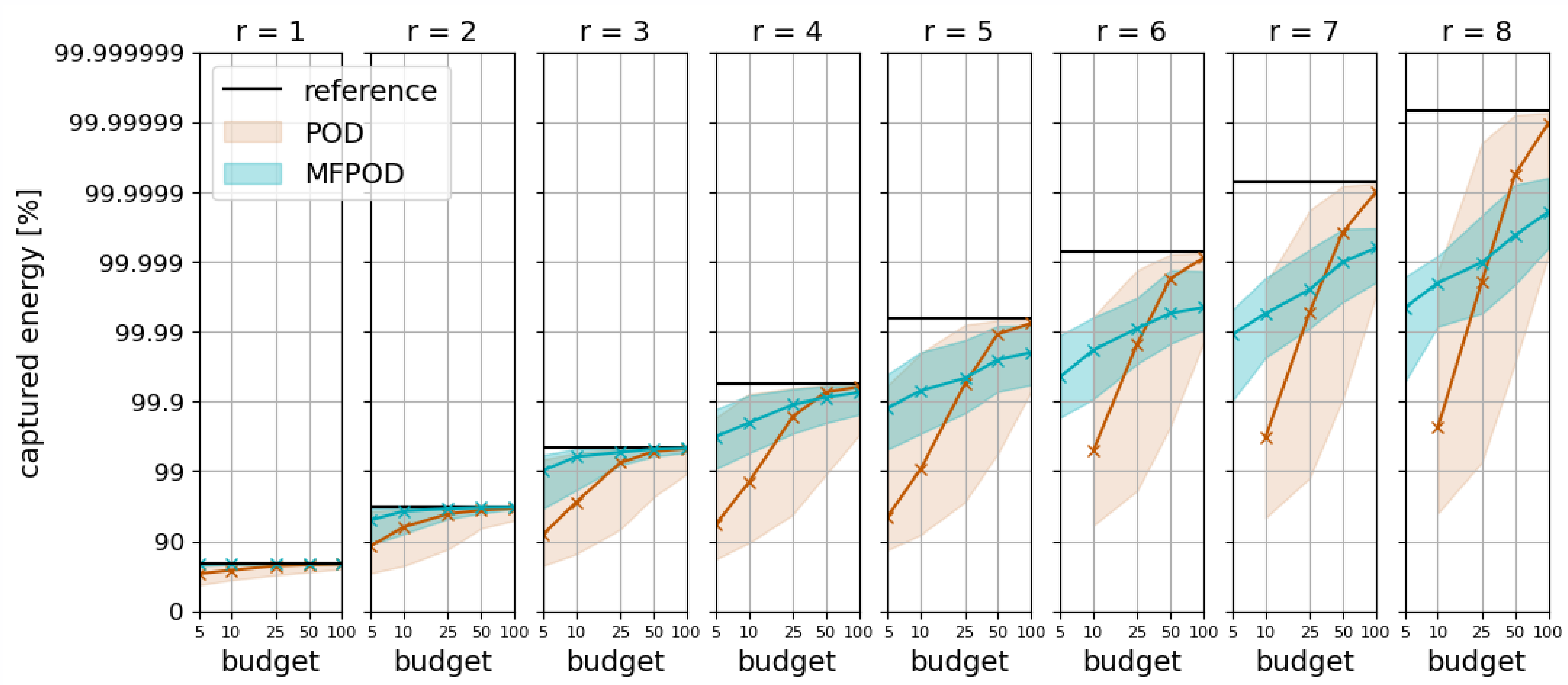

Example: Ice sheet dynamics of Pine Island Glacier

using the Ice-sheet and Sea-level System Model (ISSM)

High-fidelity: Higher-order (HO) model

$$\nabla \cdot (2\mu \dot{\varepsilon}_{\mathrm{HO},1}) = \rho_{\mathrm{ice}} g \frac{\partial s}{\partial x}, \qquad \nabla \cdot (2\mu \dot{\varepsilon}_{\mathrm{HO},2}) = \rho_{\mathrm{ice}} g \frac{\partial s}{\partial y},$$

where the strain rates are given by

$$\dot{\varepsilon}_{\mathrm{HO},1} = \begin{pmatrix} 2\frac{\partial v_x}{\partial x} + \frac{\partial v_y}{\partial y} \\ \frac{1}{2}\frac{\partial v_x}{\partial y} + \frac{1}{2}\frac{\partial v_y}{\partial x} \\ \frac{1}{2}\frac{\partial v_x}{\partial z} \end{pmatrix} \qquad \dot{\varepsilon}_{\mathrm{HO},2} = \begin{pmatrix} \frac{1}{2}\frac{\partial v_x}{\partial y} + \frac{1}{2}\frac{\partial v_y}{\partial x} \\ \frac{\partial v_x}{\partial x} + 2\frac{\partial v_y}{\partial y} \\ \frac{1}{2}\frac{\partial v_y}{\partial z} \end{pmatrix}$$

and the basal boundary conditions are

$$2\mu \dot{\varepsilon}_{\mathrm{HO},1} \cdot \mathbf{n} = -\beta^2 N v_x \qquad 2\mu \dot{\varepsilon}_{\mathrm{HO},2} \cdot \mathbf{n} = -\beta^2 N v_y$$

Uncertain basal friction field β:

$$\theta := \log \beta \sim \mathcal{N}(\log(\beta_0), C)$$

(discretized dimension 10,350)

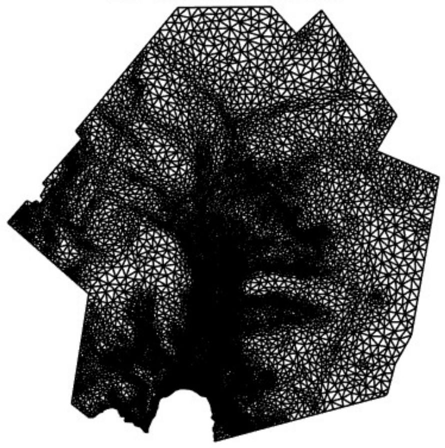

spatial discretization:
10,350 dof in each layer
x 10 vertical layers

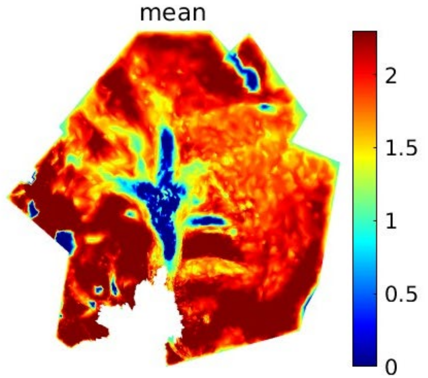

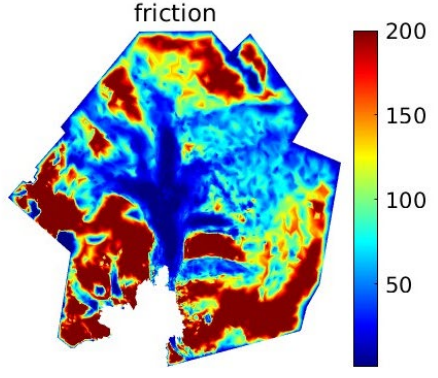

Example: Ice sheet dynamics of Pine Island Glacier

using the Ice-sheet and Sea-level System Model (ISSM)

Low-fidelity: Shallow shelf approximation (SSA) for depth-averaged velocity components

$$\overline{v}_x(x,y) \approx \frac{1}{h(x,y)} \int_{z=b(x,y)}^{s(x,y)} v_x(x,y,z)dz, \quad \overline{v}_y(x,y) \approx \frac{1}{h(x,y)} \int_{z=b(x,y)}^{s(x,y)} v_y(x,y,z)dz$$

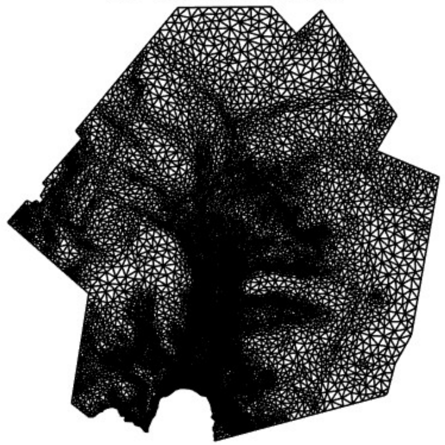

spatial discretization:
10,350 dof

Uncertain basal friction field β appears as a forcing term in SSA governing equations

Low-fidelity model is worst case 72x faster to solve than high-fidelity model (average speedup 102x)

Reference POD basis computed using 10,000 high-fidelity snapshots

Example: Ice sheet dynamics of Pine Island Glacier

using the Ice-sheet and Sea-level System Model (ISSM)

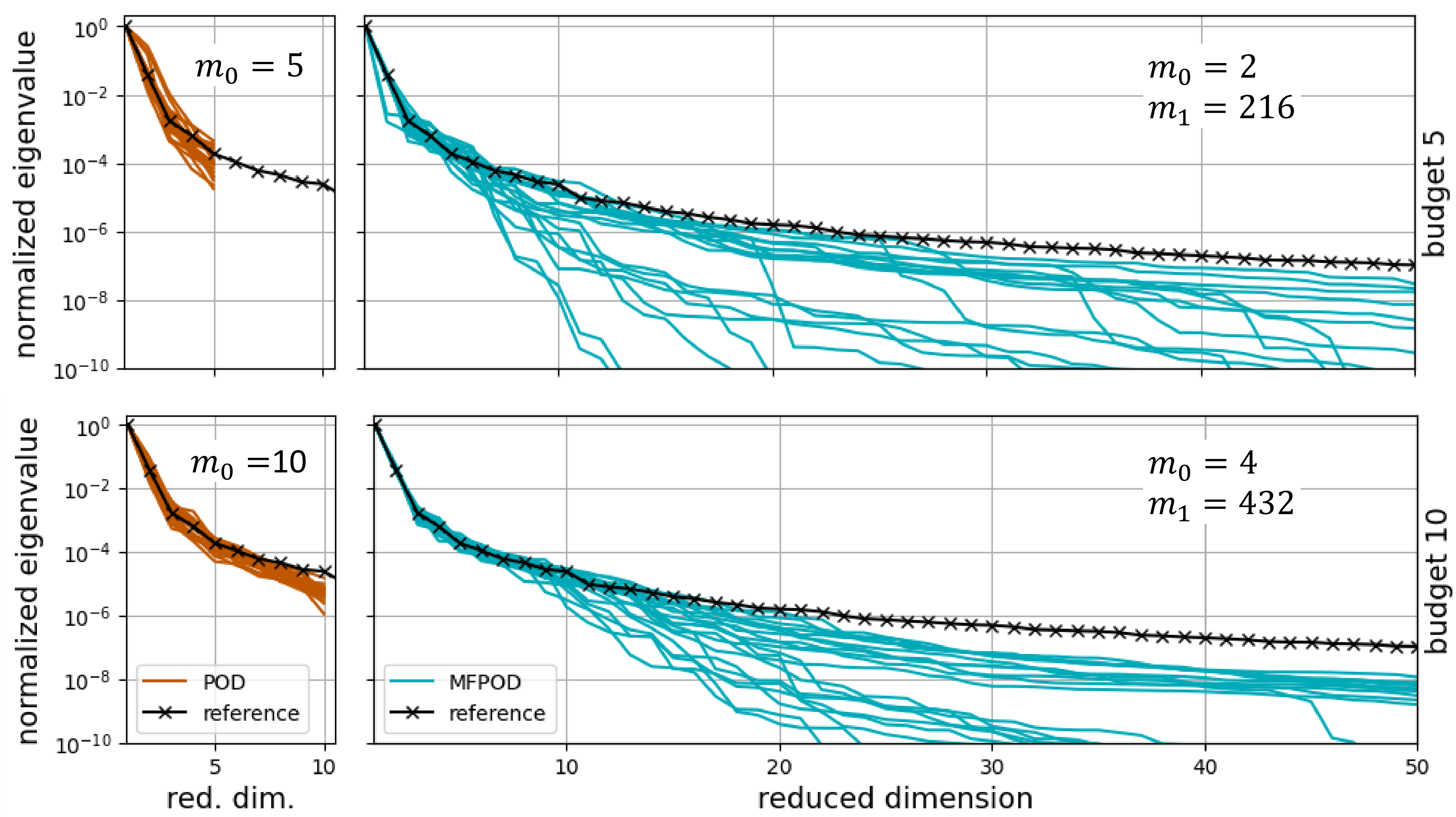

Example: Ice sheet dynamics of Pine Island Glacier

using the Ice-sheet and Sea-level System Model (ISSM)

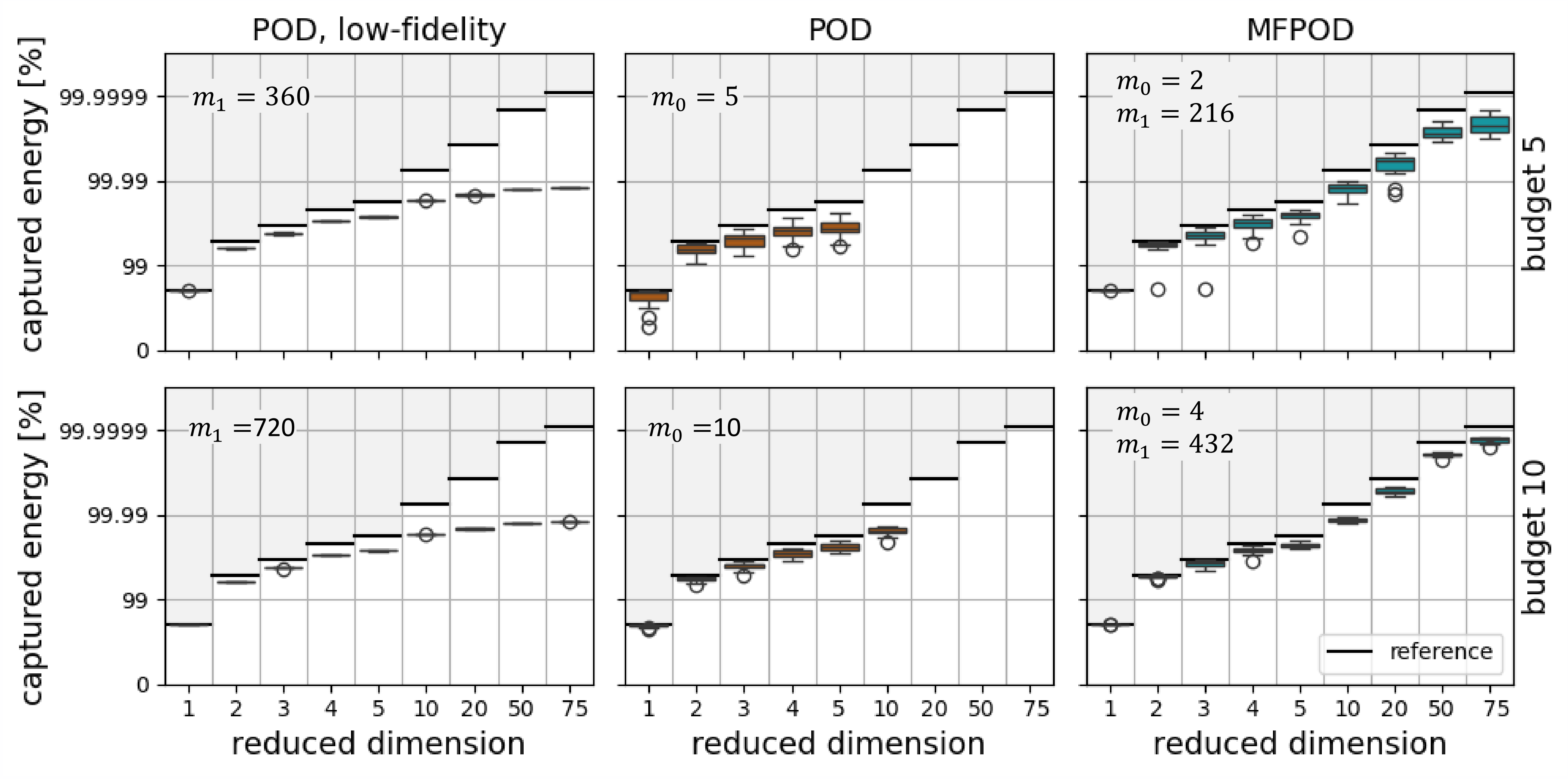

Example: Ice sheet dynamics of Pine Island Glacier
using the Ice-sheet and Sea-level System Model (ISSM)

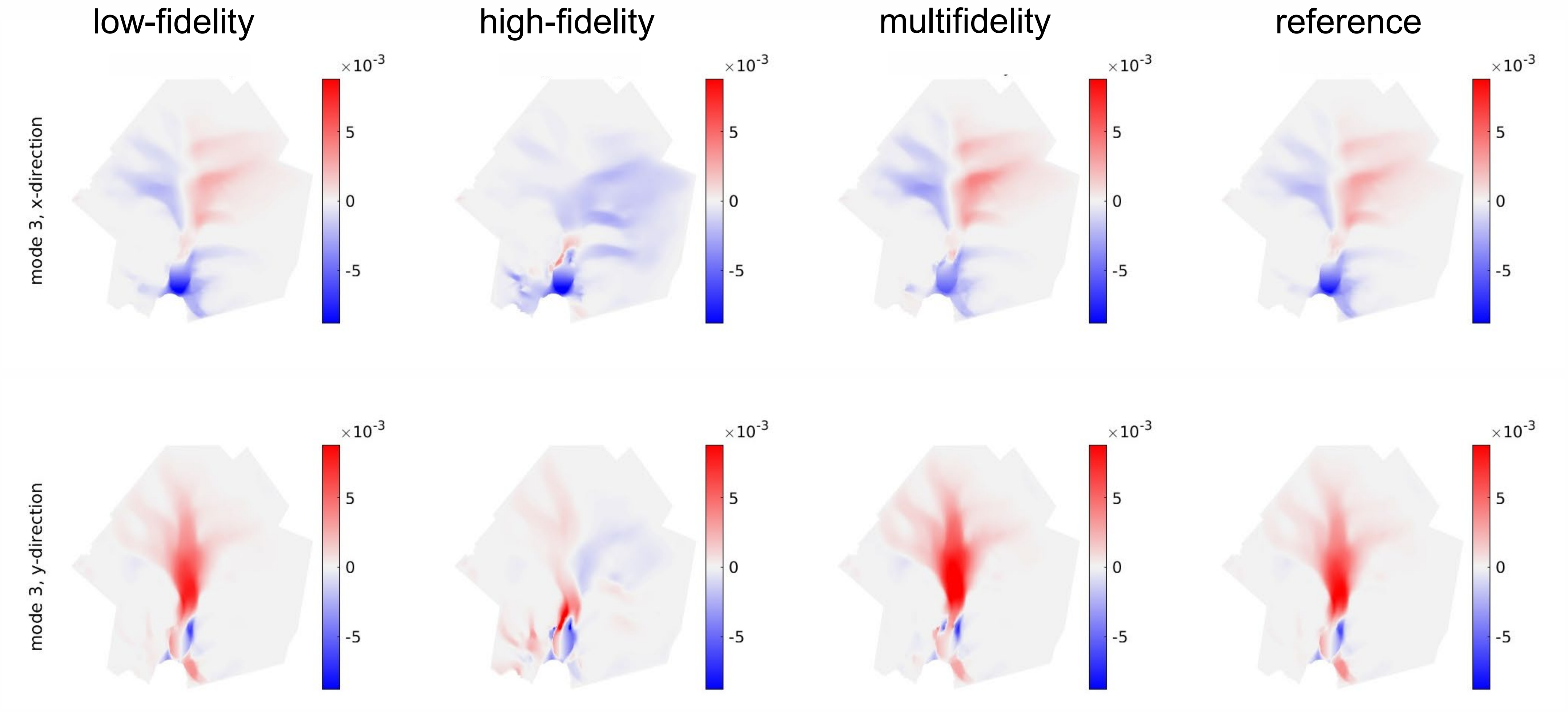

Depth-averaged velocity fields of POD mode 3

Summary

- Multifidelity POD addresses the expense of generating training data.
- It has the potential provide orders of magnitude in computational speedups together with theoretical guarantees of accuracy.
- Open questions: optimal sample allocation and control variate coefficients.
- We have derived theory for the parametric sampling case; current work is considering the time-dependent case.

Aretz, N. and Willcox, K.
Multifidelity proper orthogonal decomposition
arXiv:2605.29213, 2026